

Reactivity and Structural Aspects of Cesium and Oxygen States at Cu(110) Surfaces: An XPS and STM Investigation[†]

Albert F. Carley, Philip R. Davies, K. R. Harikumar,[‡] Rhys V. Jones,[‡] and M. Wyn Roberts*

School of Chemistry, Cardiff University, P.O. Box 912, Cardiff CF10 3TB, UK

Received: February 5, 2004; In Final Form: May 18, 2004

Structural and reactivity aspects of Cu(110)–Cs and Cu(110)–Cs/O overlayers have been investigated by XPS and STM. The development of cesium-induced structures at a Cu(110)–Cs overlayer has been followed as a function of cesium coverage at 295 K and the reactivity of the overlayer first to oxygen and subsequently to ammonia and carbon dioxide studied. For cesium concentrations up to $1.3 \times 10^{14} \text{ cm}^{-2}$ an incommensurate pseudo square structure is observed which is in registry with the copper substrate in the $\langle 100 \rangle$ direction. This coexists, at $1.3 \times 10^{14} \text{ Cs adatoms cm}^{-2}$, with a structure consisting of $\langle 1\bar{1}0 \rangle$ -orientated rows which are not atomically resolved but have a spacing in the $\langle 100 \rangle$ direction of 1.1 nm. At a cesium concentration of $1.5 \times 10^{14} \text{ cm}^{-2}$, patches of structure with an inter-row spacing of 0.7 nm are present, and at a cesium concentration of $1.9 \times 10^{14} \text{ cm}^{-2}$, only the latter spacing is observed. An increase in cesium concentration to $2.1 \times 10^{14} \text{ cm}^{-2}$ results in an increase in the inter-row spacing to 1.1 nm. Exposure of cesium-modified surfaces to oxygen results in the development of new terraces superimposed upon the cesium-modified surface with the latter structurally unchanged by the formation of the oxygen adlayer, although there is a change in the XP binding energy of the Cs(3d) peaks. The new terraces consist of $\langle 100 \rangle$ -orientated chains similar to those observed at unmodified Cu(110) surfaces; however, at low cesium concentrations these chains are arranged in (3×1) as well as (2×1) domains and at high cesium concentrations a $c(6 \times 2)\text{O}$ structure develops with an exposure of oxygen as low as 10 L. The adsorption of cesium at partially preoxidized surfaces results in the formation of a $c(2 \times 4)$ structure and also structures which have no simple relationship with the substrate lattice and which we assign to strained Cu–O (2×1) structures. At a surface with a complete monolayer of oxygen present the cesium forms $\langle 1\bar{1}0 \rangle$ chains with a minimum interchain spacing of 0.5 nm and alternate chains showing well-resolved maxima with a spacing of 0.5 nm. The adatoms in between the chains are less well-defined suggesting a degree of mobility in the $\langle 1\bar{1}0 \rangle$ direction. In comparison with oxygen at unmodified Cu(110) surfaces, oxygen states at the cesium-modified surface are unreactive to ammonia at 295 K, reaction only occurring after exposures of 300 L at 490 K. However, the cesium surface is reactive to carbon dioxide chemisorption at 295 K resulting in a surface carbonate with extensive migration of cesium and the emergence of areas of the underlying copper surface.

Introduction

The specificity of oxygen states at metal surfaces has been recognized for over two decades and has been demonstrated in a variety of systems with attention focused on the role of oxygen transients in controlling reaction pathways and attention drawn to the relationship between charge and reactivity of these states.^{1–4} The cesium/Cu(110) system is interesting in this respect because of an earlier observation that cesium present at Cu(110) surfaces perturbed the electronic state of chemisorbed oxygen so that its reactivity toward CO_2 was enhanced, mimicking that characteristic of oxygen transients.⁵ However, the reactivity of these states toward other molecules has not been investigated. At cesium surfaces four chemisorbed oxygen states have been identified⁶ by X-ray photoelectron spectroscopy (XPS). One of these, assigned as $\text{O}^{\delta-}$ and present at low surface coverage, was shown to be the active site in the oxidation of carbon monoxide to the anionic species $\text{CO}_2^{\delta-}$, the precursor

to carbonate formation. For ethene and propene oxidation at cesium and cesium-modified Ag(100) surfaces two reaction pathways were recognized, depending on whether oxygen was preadsorbed or present as one of the components of a hydrocarbon mixture,^{7,8} but the precise electronic and structural nature of the oxygen states effecting total oxidation (carbonate formation) or the formation of chemisorbed oxygenates was not established. That metastable oxygen states are present at cesium surfaces was also evident from Ertl's observations⁹ of the emission of O^- ions during oxygen chemisorption.

There has been considerable interest in the structure of alkali metal adlayers which is reviewed comprehensively by Diehl and McGrath.¹⁰ The Cu(110)–Cs surface has been studied by low-energy electron diffraction (LEED)^{11–13} and by scanning tunneling microscopy (STM)^{14,15} and shown to be similar to the Cu(110)–K system; at room temperature alkali metal adsorption results in the formation of a series of missing copper row structures described as (1×3) and (1×2) with the alkali metal believed to be situated in the missing rows. According to the LEED studies^{11,13} a “high coverage” (1×3) structure is formed at higher cesium coverages. The oxidation of potassium-modified Cu(110) surfaces has been studied by STM,¹⁴ a

[†] Part of the special issue “Gerhard Ertl Festschrift”.

* Corresponding author. E-mail: robertsmw@cf.ac.uk. Fax: +44 (0)29 2087 4030.

[‡] Present address: University of Toronto, Lash Miller Chemical Laboratories, Dept. of Chem., 80 St George St, Toronto, ON M5S 3H6, Canada.

defective (2×1)O(a) structure developing at the expense of the (1×2) potassium-induced structure, but there is no structural information available on the oxygen states at cesium-modified surfaces. It is against this background that we initiated studies of the structure and reactivity of cesium-modified Cu(110) surfaces using XPS and STM.

Experimental Section

Experiments were conducted using a combined variable temperature STM/XPS instrument (Omicron Vacuum Physik) with a base pressure of 2×10^{-10} mbar, described in detail elsewhere.¹⁶ All XP spectra were recorded with a pass energy of 50 eV resulting in typical peak half-widths of ca. 1.8 eV. Spectra were obtained by the combination of 10–20 individual scans over a 25 eV wide region, with a total acquisition time of between 10 min (Cs(3d) and Cu(2p) spectra) and 20 min (C(1s) spectra). The spectra were calibrated to the clean Cu(2p_{3/2}) peak at 932.7 eV. XPS data were acquired using commercial software (Spectra, Ron Unwin) and analyzed using software developed in-house. Surface concentrations were calculated from photoelectron peak areas according to the method discussed in detail by Carley and Roberts.¹⁷ STM images were analyzed using WSxM;¹⁸ tunneling conditions, i.e., sample bias (V_s) and tunneling current (I_t), are given in the figure legends.

The dimensions of the sample were 7 mm \times 7 mm with a thickness of approximately 0.5 mm; it was cut to within 0.5° of the (110) plane and polished mechanically down to 0.25 μ m. The sample was clamped in the sample holder and heated with a PBN heating element in the sample holder. Cleaning involved cycles of Ar⁺ sputtering (0.65 keV, 20 μ A cm⁻² for 10 min) and annealing for 40 min at 700 K. This resulted in flat terraces approximately 10–20 nm wide. Sample cleanliness was checked by XPS. Oxygen (Argo Ltd, 99.998%), nitric oxide (BDH Chemical Ltd, 99.0%), ammonia (Argo Ltd, 99.98%), and carbon dioxide (Argo Ltd, 99.995%) were used as received, gas purity being monitored with in situ mass spectrometry. Cesium was deposited using a thoroughly degassed getter (SAES).

Results and Discussion

Cesium Adsorption at a Cu(110) Surface. The formation of a cesium overlayer at a Cu(110) surface at 295 K was followed by STM as a function of cesium coverage, the latter being calculated from the areas of the Cu(2p_{3/2}) and Cs(3d) peaks in the photoelectron spectrum. The binding energy of the Cs(3d_{5/2}) photoelectron peak at the clean copper surface was 725.6 eV and was invariant with coverage.¹⁹ Figure 1 shows images observed at five cesium atom coverages, 0.85×10^{14} cm⁻², 1.3×10^{14} cm⁻², 1.5×10^{14} cm⁻², 1.9×10^{14} cm⁻², and 2.1×10^{14} cm⁻².

At the lowest coverage, Figure 1a, the surface is poorly imaged, but some islands of local order are observed and poorly resolved structures orientated in the $\langle 1\bar{1}0 \rangle$ direction are also present. Increasing the cesium coverage to 1.3×10^{14} cm⁻² leads to increased order at the surface, and two coexisting structures are observed, Figure 1b. The structure in the lower right-hand side of the image consists of rows in the $\langle 1\bar{1}0 \rangle$ direction separated by 1.1 nm (3 times the unreconstructed copper lattice spacing). This is consistent with the “low coverage” (1×3) reconstruction that has been reported by LEED¹¹ although the spacing in the $\langle 1\bar{1}0 \rangle$ direction could not be resolved. The other structure present at this concentration of cesium has not been reported in previous studies of the system but is the same as that observed in islands at lower cesium

concentrations; it is shown in more detail in Figure 2 (a and b) accompanied by a line profile (Figure 2c). The spacing of maxima in the $\langle 100 \rangle$ direction is 0.72 nm which is in close registry with the substrate copper atoms, and 0.36 nm in the $\langle 1\bar{1}0 \rangle$ direction which is not. There are irregular height differences in the $\langle 1\bar{1}0 \rangle$ direction with a maximum corrugation amplitude of 0.02 nm. The structure can be described by a pseudo square lattice with a side length of 0.5 nm rotated by 45° to the substrate; a model is shown in Figure 2d. From the STM image the concentration of sites giving rise to maxima within the structure is calculated to be 3.9×10^{14} cm⁻² which is far in excess of the average cesium concentration measured by XPS suggesting that the maxima in the STM image are due to copper atoms in a reconstructed surface. However, we are unable to rule out the possibility that the pseudo square lattice occurs in an area of locally very high cesium concentration.

The pseudo square structure is not observed at higher cesium concentrations, and at 1.5×10^{14} cm⁻² the surface is dominated by the row structure with the 1.1 nm spacing, Figure 1c. This is in good agreement with LEED^{11–13} and STM^{14,15} studies which report the “low coverage” (1×3) phase at coverages between 0.12 and 0.14 monolayers (corresponding to cesium atom concentrations of between 1.3×10^{14} and 1.5×10^{14} cm⁻²). The difficulty of resolving the atomic structure within the cesium rows suggests mobility in the $\langle 1\bar{1}0 \rangle$ direction; this would be consistent with the XP concentration data which implies an average of less than half a cesium adatom in each (1×3) unit cell.

At a cesium concentration of 1.5×10^{14} cm⁻², the “low coverage” (1×3) structure coexists with regions in which the rows are separated by only 0.7 nm, 2 times the substrate lattice spacing and at a cesium concentration of 1.9×10^{14} cm⁻², Figure 1d, only the latter row spacing is observed. A (1×2) structure was reported by LEED^{11,13} although these studies suggested a coverage range of 2.2 – 3.3×10^{14} cm⁻². The present results, Figure 1e, show that increasing the cesium concentration to 2.1×10^{14} cm⁻² results in an increase in the row spacing to 1.1 nm consistent with a “high coverage” (1×3) structure reported by LEED^{11,13} for concentrations above 3.3×10^{14} . We cannot account for the differences between the cesium structure concentration limits observed here and those reported previously,^{11,13} but it may be due to the different sensitivities of Auger (which was used in the earlier study) and XPS and Auger peak shape changes at higher cesium coverages.

Chemisorption of Oxygen at a Cu(110)–Cs Surface. The chemisorption of oxygen at 295 K was studied at different cesium concentrations corresponding to the “pseudo square”, (1×3) and (1×2) structures. The XP spectra in Figure 3 show that, irrespective of the initial cesium concentration, oxygen adsorption results in a peak in the O(1s) region at a binding energy of 529.3 eV, 0.5 eV lower than that observed at the Cu(110) surface in the absence of cesium. The cesium Cs(3d) peaks are also shifted downward in binding energy by 0.5 eV in relation to the Cu(2p_{3/2}) peak. For the lowest concentration of cesium investigated, $\sigma_{\text{Cs}} = 1.3 \times 10^{14}$ cm⁻², the STM images in Figure 4a show that an exposure of 2.3 L (1 L = 10^{-6} Torr s, 1 mbar = 0.76 Torr) of oxygen at 295 K leads to the development, in some areas of the sample, of a similar (2×1)O(a) phase to that observed at Cu(110) surfaces in the absence of cesium.

Adsorption is however localized, since on other areas of the sample the (1×3) cesium structure is still clearly imaged. At a cesium concentration of 1.5×10^{14} cm⁻², exposure to 43 L of oxygen results in an oxygen concentration of 3.2×10^{14}

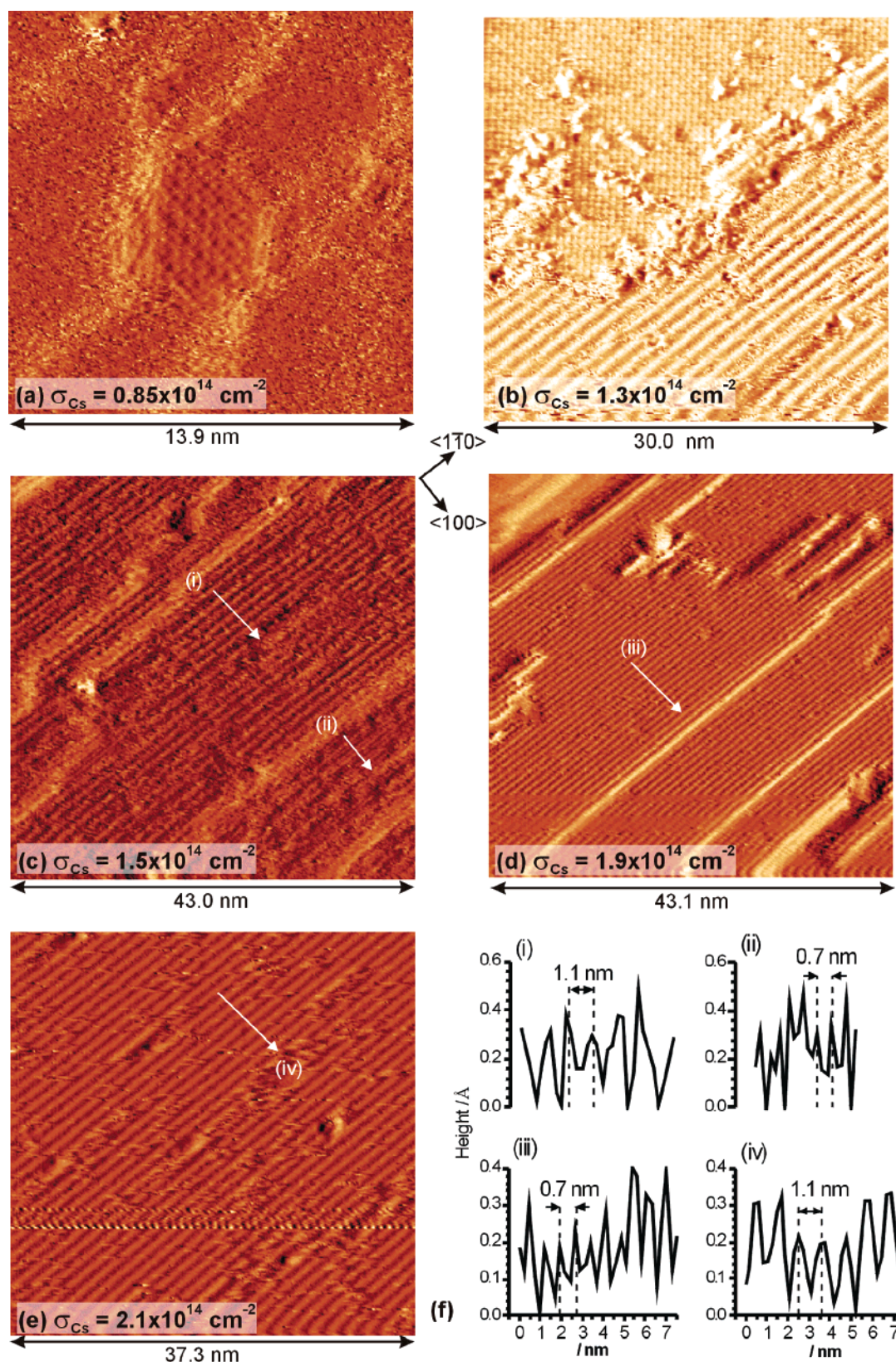


Figure 1. STM images of Cs(a) as a function of coverage at a Cu(110) surface at 295 K. (a) Island of pseudo square structure $\sigma_{\text{Cs}} = 0.85 \times 10^{14} \text{ cm}^{-2}$. $V_{\text{S}} = -0.109 \text{ V}$, $I_{\text{T}} = 3.28 \text{ nA}$. (b) Coexisting pseudo square and “low coverage” (1×3) structure, $\sigma_{\text{Cs}} = 1.30 \times 10^{14} \text{ cm}^{-2}$. $V_{\text{S}} = -0.64 \text{ V}$, $I_{\text{T}} = 3.41 \text{ nA}$. (c) Coexisting (1×3) and (1×2) structures, $\sigma_{\text{Cs}} = 1.5 \times 10^{14} \text{ cm}^{-2}$. $V_{\text{S}} = -0.58 \text{ V}$, $I_{\text{T}} = 3.28 \text{ nA}$. (d) (1×2) structure, $\sigma_{\text{Cs}} = 1.9 \times 10^{14} \text{ cm}^{-2}$. $V_{\text{S}} = 0.75 \text{ V}$, $I_{\text{T}} = 3.11 \text{ nA}$. (e) “High-coverage” (1×3) structure, $\sigma_{\text{Cs}} = 2.1 \times 10^{14} \text{ cm}^{-2}$. $V_{\text{S}} = 2.31 \text{ V}$, $I_{\text{T}} = 2.83 \text{ nA}$. (f) Line profiles from images c, d, and e.

cm^{-2} , and the STM images Figure 4b shows the coexistence of domains of (2×1) and (3×1) structures. In addition, in a different area of the surface (inset in image b), there is evidence for more complex structural features with chains, $\sim 2.5 \text{ nm}$ in

length, running at an angle to the main structures. On the basis of the observations made below for oxygen adsorption at a surface with a higher initial cesium concentration, we assign these features to localized areas of a $c(6 \times 2)$ structure.

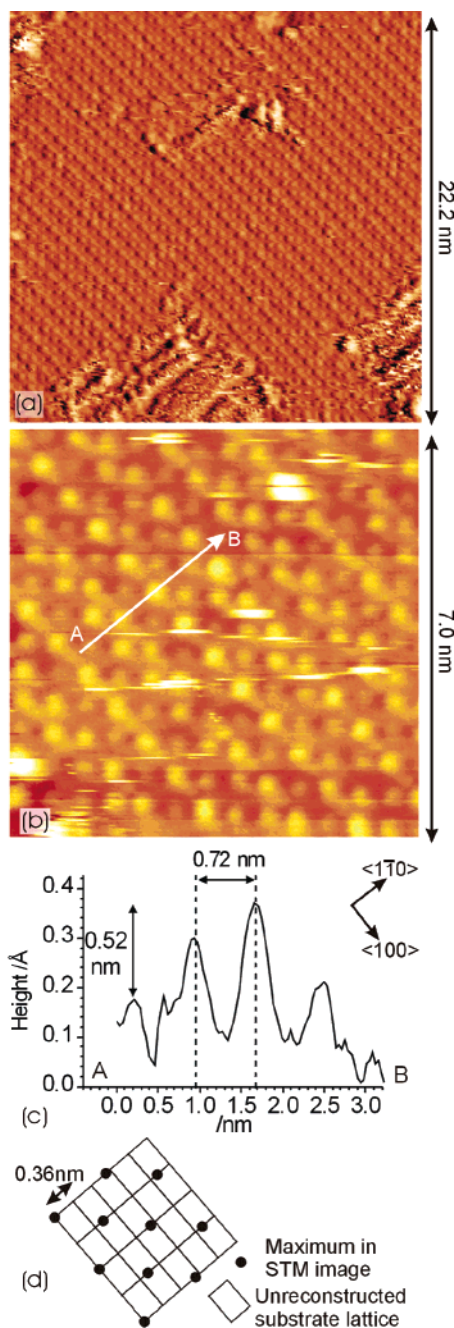


Figure 2. Close up of the pseudo square structure seen at low cesium coverages in Figure 1b, $\sigma_{\text{Cs}} = 1.3 \times 10^{14} \text{ cm}^{-2}$. (a) $V_{\text{S}} = -0.57 \text{ V}$, $I_{\text{T}} = 2.69 \text{ nA}$. (b) $V_{\text{S}} = -0.35 \text{ V}$, $I_{\text{T}} = 3.28 \text{ nA}$. (c) Line profile across the structure in (b) showing height variations between the rows. (d) Model comparing the observed structure to the unreconstructed Cu(110) lattice.

When the initial cesium concentration is $1.9 \times 10^{14} \text{ cm}^{-2}$, and the surface covered by a complete (1×2) structure, a 10 L oxygen exposure results in the development of extensive areas of a $c(6 \times 2)$ structure, Figure 4d, mixed with limited areas of (2×1) structure. In the absence of cesium, the former is observed at clean Cu(110) surfaces only after exposures to oxygen of 10 000 L.^{20,21} The presence of the cesium therefore accelerates structure development, and this is a function of cesium concentration. We have discussed previously^{2,22–24} the role of transients in oxidation processes and shown in several systems that increasing the stability of transient species by forming them at low temperatures can increase oxidation rates. In particular, the $c(6 \times 2)$ oxygen structure was formed²⁵ at a

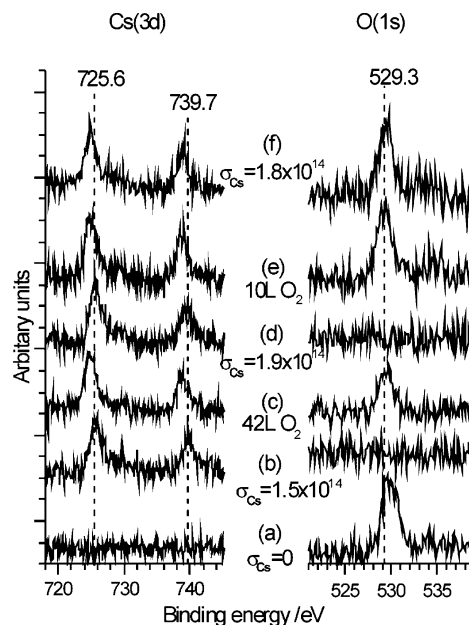


Figure 3. XP O(1s) and Cs(3d) spectra of the interaction of oxygen and cesium at Cu(110) surfaces at 295 K. (a) After exposing a clean Cu(110) surface to 50 L of $\text{O}_2(\text{g})$, $\sigma_{\text{O}} = 4.6 \times 10^{14} \text{ cm}^{-2}$. (b) $\sigma_{\text{Cs}} = 1.5 \times 10^{14} \text{ cm}^{-2}$. (c) Surface in (b) exposed to 42 L of $\text{O}_2(\text{g})$. $\sigma_{\text{Cs}} = 1.5 \times 10^{14} \text{ cm}^{-2}$, $\sigma_{\text{O}} = 3.2 \times 10^{14} \text{ cm}^{-2}$. (d) Cesium adsorbed at a clean surface, $\sigma_{\text{Cs}} = 1.9 \times 10^{14} \text{ cm}^{-2}$. (e) Surface in (d) exposed to 10 L of $\text{O}_2(\text{g})$ $\sigma_{\text{Cs}} = 1.9 \times 10^{14} \text{ cm}^{-2}$, $\sigma_{\text{O}} = 4.2 \times 10^{14} \text{ cm}^{-2}$. (f) Deposition of cesium on a partially oxygen-covered Cu(110) surface, $\sigma_{\text{Cs}} = 1.8 \times 10^{14} \text{ cm}^{-2}$, $\sigma_{\text{O}} = 4.4 \times 10^{14} \text{ cm}^{-2}$.

Cu(110) surface after warming a disordered oxygen state created by an exposure of a few langmuir at 80–295 K

The development of the oxygen adlayer at a cesium-modified surface during exposure to oxygen at a pressure of 3×10^{-8} mbar was followed by STM, and a sequence of images recorded at the same area of the surface is shown in parts a–f of Figure 5. The initial cesium concentration was $1.5 \times 10^{14} \text{ cm}^{-2}$, resulting in a (1×3) surface structure, Figure 5a. Images b–f were recorded after 150, 270, 480, 930, and 1830 s exposure to dioxygen, respectively. The cesium-induced (1×3) structure can be clearly observed in (a), but with increasing exposure to oxygen the development of new terraces containing rows running in the $\langle 100 \rangle$ direction becomes apparent. These terraces appear to develop on top of the original cesium-induced structure, and this impression is reinforced when the sample is imaged with different tunneling conditions. For example, parts e and f of Figures 4 show the same area of the surface after a (1×2) cesium structure has been exposed to oxygen forming a $(2 \times 1)\text{O}(\text{a})$ structure. Figure 4e was recorded with a sample bias of -2 V and clearly shows the $(2 \times 1)\text{O}(\text{a})$ structure with the characteristic Cu–O chains running in the $\langle 100 \rangle$ direction. Figure 4f was recorded immediately afterward with a sample bias of -1 V , and under these conditions the original (1×2) cesium-induced structure is imaged.

We conclude that the $(2 \times 1)\text{O}(\text{a})$ adlayer has been formed without perturbing the cesium-induced structure, presumably through the abstraction of copper atoms from step edges. This behavior is markedly different from that reported¹⁴ for the oxidation of potassium-modified Cu(110) surfaces where oxygen adsorption leads to the disintegration of the (1×2) potassium-induced structure due to the extraction of copper atoms from the terraces by oxygen transients. We cannot determine directly from the STM which layer, the cesium or the oxygen, is on top when the cesium-covered surface is oxidized, but since the (1×2) cesium-induced structure is known^{11,12,14} to involve a

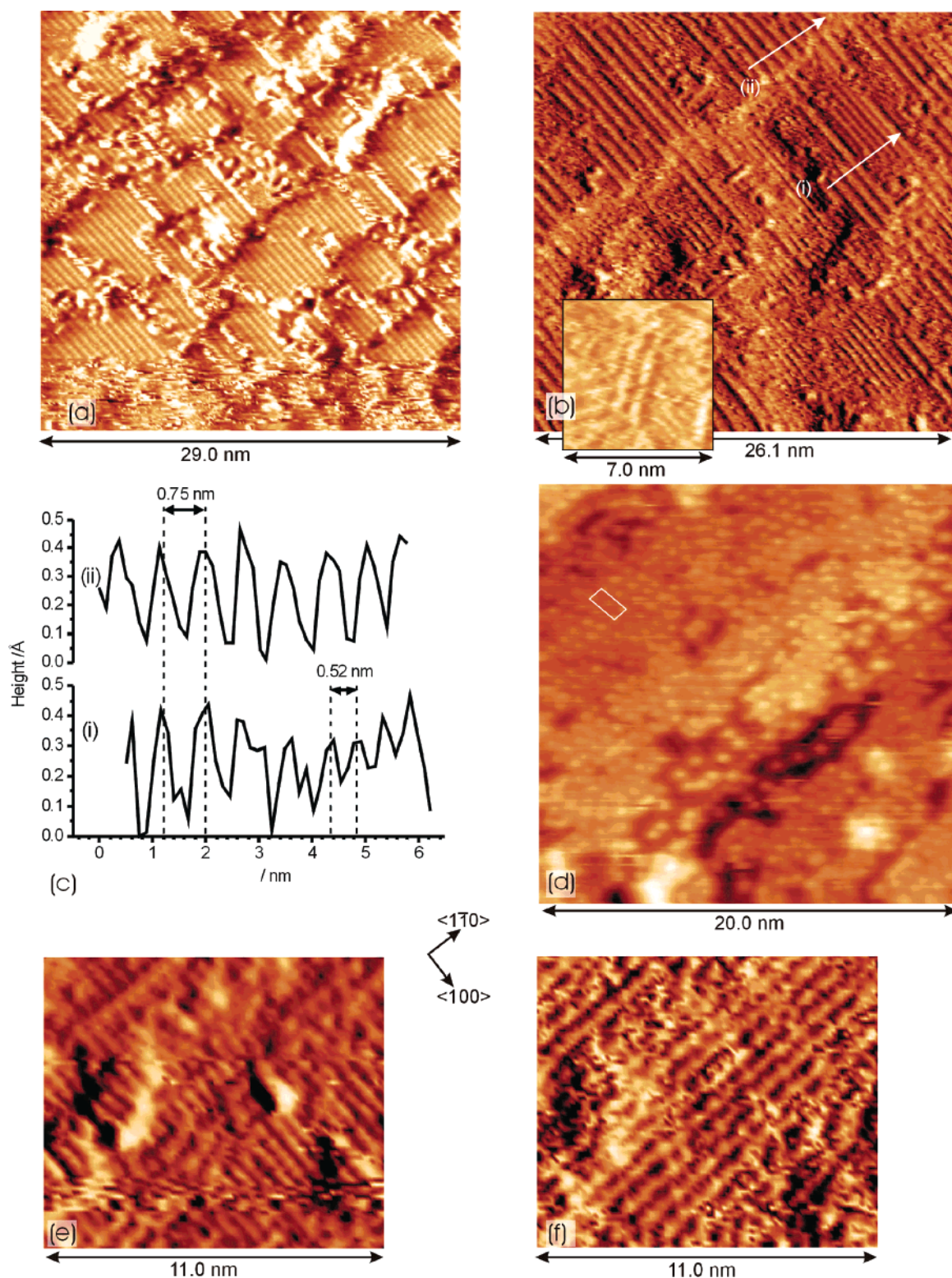


Figure 4. STM images of the adsorption of oxygen at Cu(110) surfaces with different initial cesium-induced structures. (a) $(2 \times 1)\text{O(a)}$ formed from an exposure of 2.3 L of $\text{O}_2(\text{g})$ to a surface with the pseudo square and (1×3) cesium structures ($\sigma_{\text{Cs}} = 1.3 \times 10^{14} \text{ cm}^{-2}$). The oxygen concentration is $1.6 \times 10^{14} \text{ cm}^{-2}$. $V_{\text{S}} = +1.73 \text{ V}$, $I_{\text{T}} = 2.79 \text{ nA}$. (b) (2×1) and (3×1) O(a) structures formed from an exposure of 43 L of $\text{O}_2(\text{g})$ to a surface with the “low coverage” (1×3) structure ($\sigma_{\text{Cs}} = 1.5 \times 10^{14} \text{ cm}^{-2}$). The oxygen concentration is $3.2 \times 10^{14} \text{ cm}^{-2}$. $V_{\text{S}} = -0.58 \text{ V}$, $I_{\text{T}} = 3.28 \text{ nA}$. Inset, a different area of the crystal imaged under the same conditions showing an incomplete $\text{c}(6 \times 2)\text{O(a)}$ structure. $V_{\text{S}} = -0.95 \text{ V}$, $I_{\text{T}} = 2.99 \text{ nA}$. (c) Line profiles from image b showing the (2×1) and (3×1) spacings. (d) Incomplete $\text{c}(6 \times 2)\text{O(a)}$ structure formed from exposing a surface with the (1×2) cesium-induced structure to 10 L of $\text{O}_2(\text{g})$. The $\text{c}(6 \times 2)$ unit cell is shown on the figure, $\sigma_{\text{Cs}} = 1.9 \times 10^{14} \text{ cm}^{-2}$, $\sigma_{\text{O}} = 4.2 \times 10^{14} \text{ cm}^{-2}$. (e and f) STM images of the same area of a surface in which the $(2 \times 1)\text{O(a)}$ has been formed on a cesium-induced (1×2) structure ($\sigma_{\text{Cs}} = 1.9 \times 10^{14} \text{ cm}^{-2}$, $\sigma_{\text{O}} = 4.2 \times 10^{14} \text{ cm}^{-2}$). Scans were recorded 50 s apart using different tunneling conditions, (e) $V_{\text{S}} = -2.0 \text{ V}$, $I_{\text{T}} = 3.11 \text{ nA}$, (f) $V_{\text{S}} = -0.95 \text{ V}$, $I_{\text{T}} = 3.11 \text{ nA}$, and show the continued presence of the (1×2) cesium structure underneath the $(2 \times 1)\text{O(a)}$ lattice.

missing row reconstruction of the copper substrate it is probable that the oxygen adlayer has developed superimposed on the

cesium-induced structure. However, we have also considered the alternative possibility, that the cesium migrates over the (2

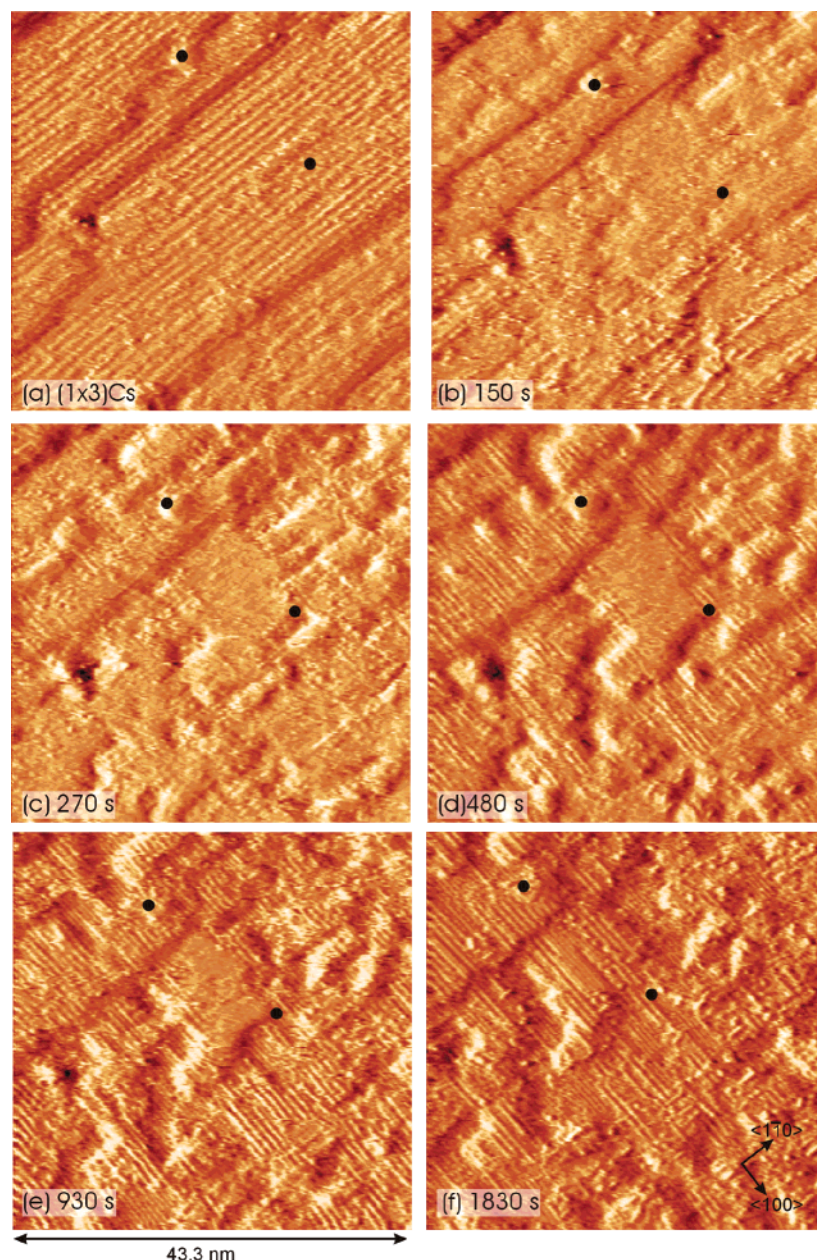


Figure 5. Sequence of STM images showing the development of the oxygen adlayer on a cesium-covered Cu(110) surface ($\sigma_{\text{Cs}} = 1.5 \times 10^{14} \text{ cm}^{-2}$) during an exposure to $\text{O}_2(\text{g})$ at 3×10^{-8} mbar and 295 K. (a) (1×3) cesium structure at surface before commencing the oxygen exposure. (b to f) were recorded using the same tunneling conditions ($V_s = -0.58$ V, $I_T = 3.28$ nA) at the following times during the exposure: (b) 150 s; (c) 270 s; (d) 480 s; (e) 930 s; (f) 1830 s. The black dots locate identical points at the surface in each image.

$\times 1$)O(a) adlayer, by investigating the adsorption of cesium on a Cu(110)–O(2×1) surface. Figure 6 shows cesium deposition on top of a partial monolayer of oxygen, Figure 6a, and a complete (2×1)O(a) adlayer, Figure 6b. In the presence of the partial oxygen monolayer ($\sigma_{\text{O}} = 1.7 \times 10^{14} \text{ cm}^{-2}$), cesium adsorption ($\sigma_{\text{Cs}} = 1.8 \times 10^{14} \text{ cm}^{-2}$) resulted in the development of well-ordered $c(2 \times 4)$ domains coexisting with structural features which have no simple relationship with either the Cu(110) substrate or the $c(2 \times 4)$ structure. They appear as “bent” rows, suggestive of a strained structure. Although, from STM, we cannot determine the atomic composition of the two different structures directly, the resemblance of the “bent” rows to the original oxygen structure strongly points to the assignment of these to strained (2×1)O(a); and the observed coverage of structures (about a third of the surface) is consistent with the concentration of oxygen calculated from the XP data. Similarly, the coverage of the $c(2 \times 4)$ structure (about two-thirds of the

surface) is consistent with the cesium concentration. The interatomic spacing of the features within the $c(2 \times 4)$ structure is 0.5 nm, close to the Cs–Cs spacing in the monolayer formed at Cu(110) surfaces at 80 K,^{11,13} though in that case a “quasihexagonal” structure was observed. The experiment suggests that the presence of the partial oxygen adlayer prevents the reconstruction of the surface and instead the cesium adsorbs directly at the Cu(110) surface.

When cesium was adsorbed ($\sigma_{\text{Cs}} = 1.8 \times 10^{14} \text{ cm}^{-2}$) at a fully oxygen-covered surface, a disordered layer resulted which prevented the imaging of the (2×1)O(a) structure. However, at higher concentrations of cesium ($2.75 \times 10^{14} \text{ cm}^{-2}$) a more ordered structure develops, Figure 6b. Under these conditions a large number of features are observed in the STM image with many organized into rows in the $\langle 110 \rangle$ direction; the interatomic spacing within each row is 0.5 nm. The minimum spacing between the row structures in the $\langle 100 \rangle$ direction is 0.7 nm,

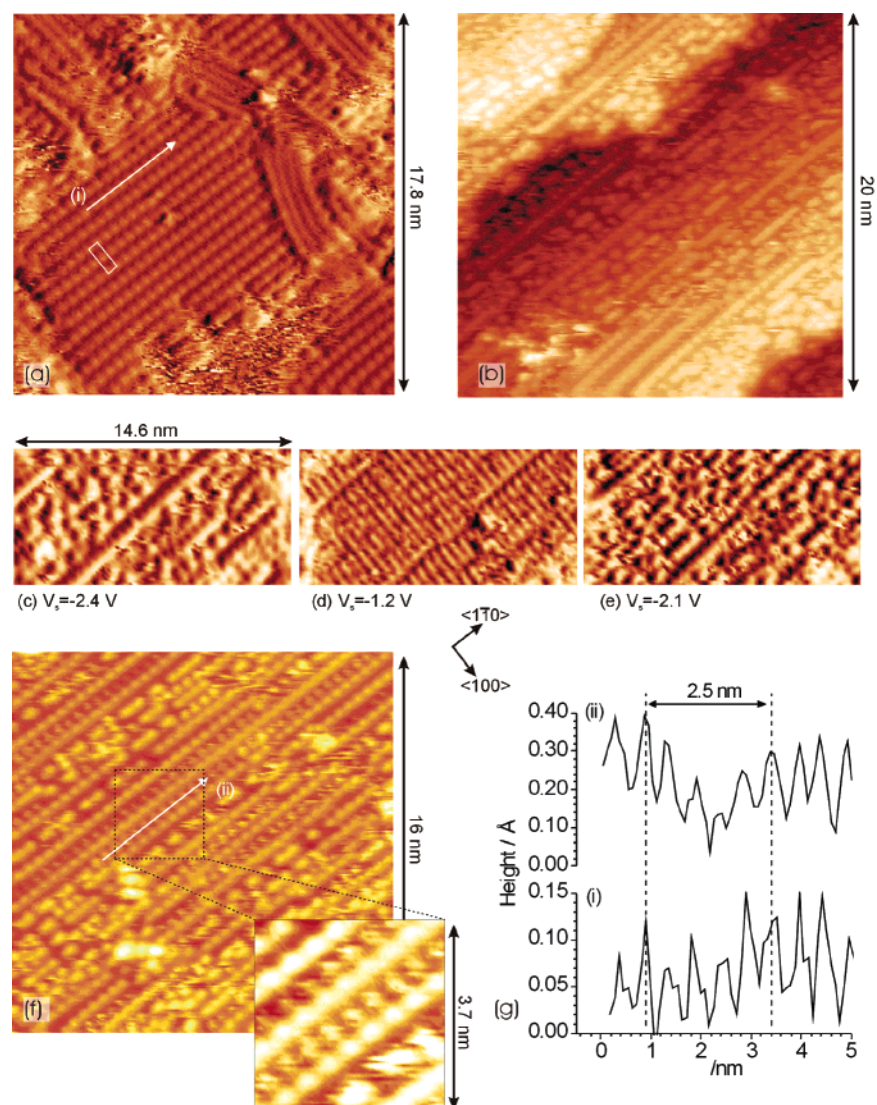


Figure 6. Adsorption of cesium at oxygen-covered Cu(110) surfaces. (a) $c(2 \times 4)$ structure and “bent” chains, formed by cesium adsorption at a surface with a partial oxygen monolayer. The $c(2 \times 4)$ unit cell is shown on the figure. $\sigma_{\text{O}} = 1.7 \times 10^{14} \text{ cm}^{-2}$, $\sigma_{\text{Cs}} = 1.8 \times 10^{14} \text{ cm}^{-2}$. $V_{\text{S}} = -1.31 \text{ V}$, $I_{\text{T}} = 3.17 \text{ nA}$. (b) Adsorption of cesium on a monolayer of oxygen at 295 K, $\sigma_{\text{Cs}} = 2.75 \times 10^{14} \text{ cm}^{-2}$, $\sigma_{\text{O}} = 4.9 \times 10^{14} \text{ cm}^{-2}$. $V_{\text{S}} = -0.95 \text{ V}$, $I_{\text{T}} = 2.50 \text{ nA}$; (c–e) STM images of the same area of the surface in (b) but scanned sequentially with different tunneling conditions, (c) showing the cesium adlayer, $V_{\text{S}} = -2.4 \text{ V}$, $I_{\text{T}} = 2.6 \text{ nA}$, (d) showing the oxygen (2×1) structure, $V_{\text{S}} = -1.1 \text{ V}$, $I_{\text{T}} = 2.7 \text{ nA}$, (e) recorded immediately after (d), showing the cesium adlayer, $V_{\text{S}} = -2.1 \text{ V}$, $I_{\text{T}} = 3.1 \text{ nA}$. (f) After annealing (b) at 500 K for 60 min, $V_{\text{S}} = -0.95 \text{ V}$, $I_{\text{T}} = 2.46 \text{ nA}$. (g) Line profiles from images a and f.

twice the substrate lattice spacing, but some of the longer row structures adopt a slightly larger spacing of 1.1 nm. As in the case of oxygen adsorbed at a cesium-covered surface we find that a change in tunneling conditions results in a dramatic change in the STM image. The images in parts c–e of Figures 6 were recorded sequentially of the same area of the sample with different tunneling conditions: in Figure 6c a high sample bias (-2.4 V) is used, and the cesium adlayer is imaged; at a lower bias (-1.1 V , Figure 6d) the oxygen adlayer is imaged (though the presence of the cesium adlayer is still apparent); returning to a higher bias (-2.1 V , Figure 6e) the cesium is once again imaged and apparently unchanged by the scanning procedure.

The adsorbed cesium adlayer was imaged more clearly after annealing to 550 K and cooling to 295 K, Figure 6f. The structure is incomplete but is again characterized by $\langle 1\bar{1}0 \rangle$ -orientated rows which show an interatom spacing of 0.5 nm, Figure 6g. In the $\langle 100 \rangle$ direction, rows are also separated by approximately 0.5 nm, resulting in every other row being out of registry with the underlying Cu(110) $(2 \times 1)\text{O(a)}$ structure;

this is probably the reason that every other row is imaged more clearly than its neighbors which is shown more clearly in the expanded part of Figure 6g.

Chemisorption of Ammonia and Carbon Dioxide at Cu(110)–Cs and Cu(110)–Cs/O Surfaces. The reactivity of oxygen toward ammonia at cesium-modified surfaces was investigated for two different concentrations of cesium and oxygen: a Cu(110)–Cs surface ($\sigma_{\text{Cs}} = 1.5 \times 10^{14} \text{ cm}^{-2}$) with an initial surface oxygen concentration of $3.2 \times 10^{14} \text{ cm}^{-2}$ and a Cu(110)–Cs surface ($\sigma_{\text{Cs}} = 1.3 \times 10^{14} \text{ cm}^{-2}$) with an initial oxygen concentration of $1.6 \times 10^{14} \text{ cm}^{-2}$, ammonia being unreactive at the modified surface in the absence of oxygen. For both oxygen concentrations studied, no reaction could be detected after ammonia exposures of 100 L at 295 K by either STM or XPS. The surface oxygen was also unreactive to a further 200 L exposure of ammonia at 390 K. However, a reaction was observed after exposing the Cu(110)–Cs surface ($\sigma_{\text{Cs}} = 1.3 \times 10^{14} \text{ cm}^{-2}$, $\sigma_{\text{O}} = 1.6 \times 10^{14} \text{ cm}^{-2}$) to ammonia (300 L) at 475 K, the resulting N(1s) spectrum showing a peak

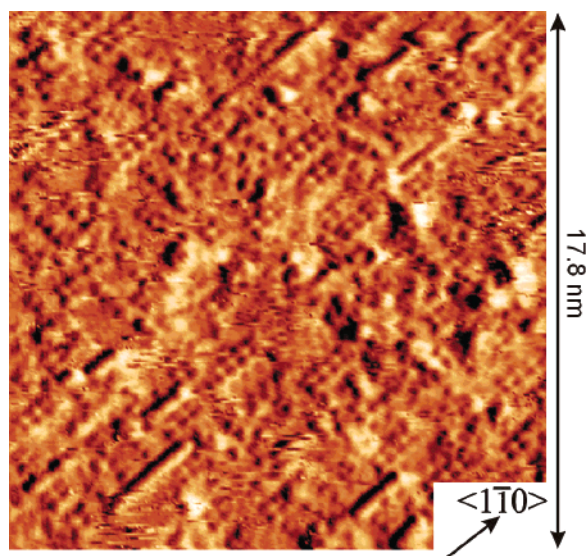


Figure 7. STM image recorded after the exposure of oxygen at a cesium-modified surface ($\sigma_{\text{Cs}} = 1.3 \times 10^{14} \text{ cm}^{-2}$, $\sigma_{\text{O}} = 1.6 \times 10^{14} \text{ cm}^{-2}$) to 300 L of $\text{NH}_3(\text{g})$ at 475 K. $V_{\text{S}} = -0.86 \text{ V}$, $I_{\text{T}} = 2.41 \text{ nA}$.

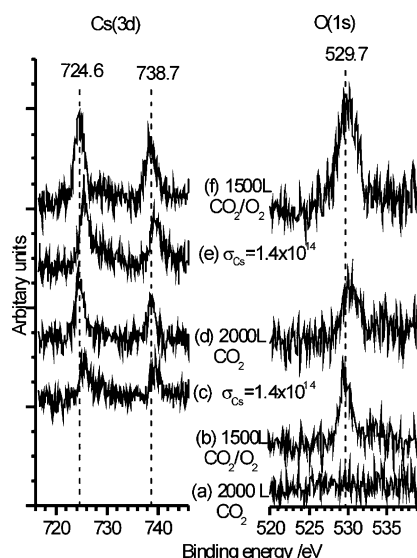


Figure 8. O(1s) and Cs(3d) XP spectra showing the interaction of carbon dioxide with clean and cesium-modified Cu(110) surfaces. (a) After exposing the clean surface to 2000 L of $\text{CO}_2(\text{g})$. (b) After exposing a clean surface to 1500 L of a 100:1 CO_2/O_2 mixture, $\sigma_{\text{O}} = 3.7 \times 10^{14} \text{ cm}^{-2}$. (c) Cesium deposited at a clean Cu(110) surface, $\sigma_{\text{Cs}} = 1.5 \times 10^{14} \text{ cm}^{-2}$. (d) After exposing the surface in (c) to 2000 L of $\text{CO}_2(\text{g})$ at 295 K, $\sigma_{\text{Cs}} = 1.5 \times 10^{14} \text{ cm}^{-2}$, $\sigma_{\text{O}} = 3.0 \times 10^{14} \text{ cm}^{-2}$. (e) Cesium deposited at a clean Cu(110) surface, $\sigma_{\text{Cs}} = 1.4 \times 10^{14} \text{ cm}^{-2}$. (f) After exposing the surface in (e) to 1500 L of a 100:1 CO_2/O_2 mixture, $\sigma_{\text{Cs}} = 1.4 \times 10^{14} \text{ cm}^{-2}$, $\sigma_{\text{O}} = 6.6 \times 10^{14} \text{ cm}^{-2}$.

at about 397 eV consistent with a mixed nitride/imide state¹ with a surface concentration of approximately 2×10^{14} nitrogen species cm^{-2} .

Although the surface is now largely disordered, there is evidence in the STM, Figure 7, for rows running in the $\langle 110 \rangle$ direction and characteristic of $\text{NH}_x(\text{a})$ species (x is between 0 and 1) at Cu(110) surfaces.²⁵ We note that under these reaction conditions a peak in the O(1s) region indicates that approximately $1 \times 10^{14} \text{ cm}^{-2}$ of oxygen remains unreacted. This contrasts sharply with the equivalent situation for oxygen adsorbed at clean Cu(110) surfaces: low oxygen concentrations undergoing a facile chemisorptive replacement reaction at room temperature with ammonia exposures of $<50 \text{ L}$, and the

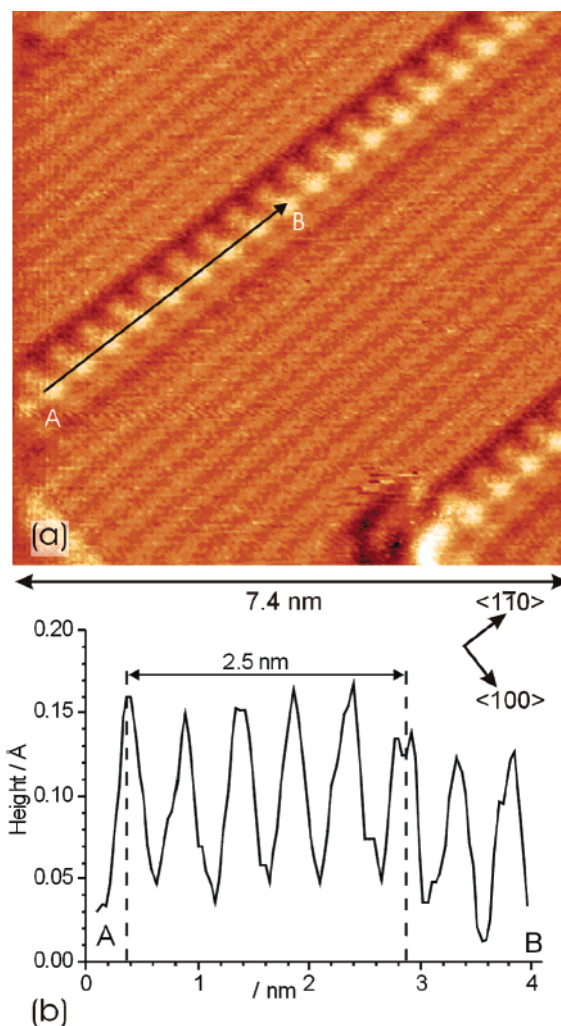


Figure 9. (a) STM image recorded after exposing a cesium-modified Cu(110) surface, $\sigma_{\text{Cs}} = 1.5 \times 10^{14} \text{ cm}^{-2}$, to 2000 L of $\text{CO}_2(\text{g})$ at 295 K. (a) Image showing the coexistence of carbonate structures and areas of “clean” Cu(110), $V_{\text{S}} = 0.70 \text{ V}$, $I_{\text{T}} = 3.10 \text{ nA}$. (b) Line profile over the carbonate structure.

comparatively unreactive saturated oxygen adlayer being completely removed by ammonia at 470 K.^{1,2}

In contrast, cesium modification results in an increased reactivity of the surface to carbon dioxide at room temperature. Figure 8 shows the XP spectra for a series of experiments at clean and cesium-modified Cu(110) surfaces. In the absence of cesium an exposure of 2000 L of CO_2 results in no adsorbed species, Figure 8a, and a surface exposed to a 1:100 O_2/CO_2 mixture at 295 K shows only chemisorbed oxygen in the XP spectra with a characteristic O(1s) peak at 529.7 eV, Figure 8b, and the $(2 \times 1)\text{O}(\text{a})$ structure in the STM images. However, exposure of a cesium-modified Cu(110) surface ($\sigma_{\text{Cs}} = 1.4 \times 10^{14} \text{ cm}^{-2}$) to carbon dioxide at 295 K results in the adsorption of an oxygen-containing species with an O(1s) binding energy of 530.8 eV and an atom concentration of $3 \times 10^{14} \text{ cm}^{-2}$. There was also a weak peak in the C(1s) spectrum at a binding energy of about 288 eV; on the basis of our earlier XP and high-resolution electron energy loss spectroscopy (HREEL) studies of this system^{5,7} these peaks are assigned to a carbonate.

When the surface was exposed to a 1:100 O_2/CO_2 mixture, Figure 8f, a composite O(1s) peak is observed consisting of components corresponding to O(a) and $\text{CO}_3(\text{a})$ in approximately a 1:1 ratio. STM images of a Cu(110)–Cs surface ($\sigma_{\text{Cs}} = 1.5 \times 10^{14} \text{ cm}^{-2}$) which has been exposed to 1500 L of carbon

dioxide at 295 K are shown in Figure 9a. Chain structures are observed orientated in the $\langle 1\bar{1}0 \rangle$ direction with a regular periodicity within the chains of 0.5 nm, Figure 9b. On the basis of the XP binding energies, these new chain structures are assigned to cesium carbonate. In addition to the carbonate structures, there are areas displaying $\langle 1\bar{1}0 \rangle$ directed rows with a 0.36 nm spacing consistent with the unreconstructed clean Cu(110) substrate.

Conclusions

Four distinct structures have been delineated at the Cu(110)–Cs interface at 295 K; for cesium concentrations between 0.85 and $1.3 \times 10^{14} \text{ cm}^{-2}$ a noncommensurate pseudo square structure forms which coexists at the upper limit with a “low coverage” (1×3) structure. The latter is present up to a cesium concentration of $1.5 \times 10^{14} \text{ cm}^{-2}$ where it coexists with a (1×2) structure. The (1×2) structure is the only state observed at a concentration of $1.9 \times 10^{14} \text{ cm}^{-2}$, but for a cesium concentration of $2.1 \times 10^{14} \text{ cm}^{-2}$ and above the surface is covered by a “high coverage” (1×3) structure. Oxygen chemisorption at the Cu(110)–Cs overlayer results in the formation of (2×1) and (3×1) domains with indications of another structure which at higher cesium coverages can be resolved into the $c(6 \times 2)$ O(a) structure. The latter is formed far more readily at the cesiated surface than at clean Cu(110) surfaces. From the STM results we have established that, in contrast to the case of potassium-modified Cu(110) surfaces, the oxygen adlayer develops on top of an essentially unchanged Cu/Cs reconstruction. The development of the (2×1) O(a) adlayer at clean Cu(110) surfaces is believed²⁶ to involve the abstraction of copper atoms from step edges by oxygen transients, which then diffuse to sites on the terraces at which the added (2×1) structure nucleates. The present results suggest that a similar process occurs at the cesium-reconstructed copper surface. Cesium adsorption at preoxidized surfaces results in the development of different structures depending on the initial oxygen concentration and cesium coverage; these are characterized by a $c(2 \times 4)$ structure at low oxygen concentrations and a (2×3) structure when cesium is adsorbed at a surface with a monolayer of oxygen adatoms. Although oxygen adsorbed at the cesium-modified Cu(110) surface forms structures that are similar to those formed at the clean Cu(110) surface, the reactivity of the oxygen is significantly reduced being unreactive toward ammonia at temperatures up to 390 K. Reaction can only be initiated by increasing the temperature to 475 K. The XP data shows a decrease in the binding energy of the oxygen adsorbed in the presence of the cesium, indicating an increase in the effective charge on the oxygen; we have noted previously^{2,7} the importance of charge on the reactivity of surface oxygen.

In contrast, reaction of the surface with carbon dioxide is more facile, with a chemisorption-induced reorganization; this is suggested to be driven by the free energy of cesium carbonate formation. A somewhat analogous observation was made by Marbach et al.²⁷ during the $\text{O}_2\text{--H}_2$ reaction at a Rh(110)–K surface, where self-organization was observed by scanning photoelectron microscopy.

References and Notes

- (1) Afsin, B.; Davies, P. R.; Pashusky, A.; Roberts, M. W.; Vincent, D. *Surf. Sci.* **1993**, *284*, 109.
- (2) Carley, A. F.; Davies, P. R.; Roberts, M. W. *Catal. Lett.* **2002**, *80*, 25.
- (3) Roberts, M. W. *Chem. Soc. Rev.* **1989**, *18*, 451.
- (4) Roberts, M. W. *Chem. Soc. Rev.* **1996**, *25*, 437.
- (5) Carley, A. F.; Roberts, M. W.; Strutt, A. J. *J. Phys. Chem.* **1994**, *98*, 9175.
- (6) Kulkarni, G. U.; Laruelle, S.; Roberts, M. W. *Chem. Commun.* **1996**, 9.
- (7) Carley, A. F.; Chambers, A.; Davies, P. R.; Mariotti, G. G.; Kurian, R.; Roberts, M. W. *Faraday Discuss.* **1996**, *105*, 225.
- (8) Carley, A. F.; Chambers, A.; Roberts, M. W.; Santra, A. K. *Isr. J. Chem.* **1998**, *38*, 393.
- (9) Greber, T.; Grobecker, R.; Morgante, A.; Bottcher, A.; Ertl, G. *Phys. Rev. Lett.* **1993**, *70*, 1331.
- (10) Diehl, R. D.; McGrath, R. *Surf. Sci. Rep.* **1996**, *23*, 43.
- (11) Fan, W. C.; Ignatiev, A. *J. Vac. Sci. Technol., A* **1989**, *7*, 2115.
- (12) Hu, Z. P.; Pan, B. C.; Fan, W. C.; Ignatiev, A. *Phys. Rev. B* **1990**, *41*, 9692.
- (13) Fan, W. C.; Ignatiev, A. *Phys. Rev. B* **1988**, *38*, 366.
- (14) Schuster, R.; Barth, J. V.; Winterlin, J.; Behm, R. J.; Ertl, G. *Phys. Rev. B: Condens. Matter* **1994**, *50*, 17456; 17462.
- (15) Schuster, R.; Barth, J. V.; Ertl, G.; Behm, R. J. *Phys. Rev. Lett.* **1992**, *69*, 2547.
- (16) Carley, A. F.; Davies, P. R.; Jones, R. V.; Harikumar, K. R.; Kulkarni, G. U.; Roberts, M. W. *Surf. Sci.* **2000**, *447*, 39.
- (17) Carley, A. F.; Roberts, M. W. *Proc. R. Soc. London, Ser. A* **1978**, *363*, 403.
- (18) WSxM. <http://www.nanotec.es>.
- (19) Rodriguez, J. A.; Clendening, W. D.; Campbell, C. T. *J. Phys. Chem.* **1989**, *93*, 5238; 5248.
- (20) Feidenhansl, R.; Grey, F.; Nielsen, M.; Besenbacher, F.; Jensen, F.; Laegsgaard, E.; Stensgaard, I.; Jacobsen, K. W.; Norskov, J. K.; Johnson, R. L. *Phys. Rev. Lett.* **1990**, *65*, 2027.
- (21) Coulman, D.; Winterlin, J.; Barth, J. V.; Ertl, G.; Behm, R. J. *Surf. Sci.* **1990**, *240*, 151.
- (22) Carley, A. F.; Davies, P. R.; Kulkarni, G. U.; Roberts, M. W. *Catal. Lett.* **1999**, *58*, 93.
- (23) Roberts, M. W. *Surf. Sci.* **1994**, *300*, 769.
- (24) Carley, A. F.; Roberts, M. W.; Yan, S. *J. Chem. Soc., Chem. Commun.* **1988**, 267.
- (25) Carley, A. F.; Davies, P. R.; Jones, R. V.; Harikumar, K. R.; Kulkarni, G. U.; Roberts, M. W. *Top. Catal.* **2000**, *11*, 299.
- (26) Jensen, F.; Besenbacher, F.; Laegsgaard, E.; Stensgaard, I. *Phys. Rev. B: Condens. Matter* **1990**, *41*, 10233.
- (27) Marbach, H.; Gunther, S.; Luerksen, B.; Gregoratti, L.; Kiskinova, M.; Imbihl, R. *Catal. Lett.* **2002**, *83*, 161.